COHERENT STRUCTURES AND ONE-DIMENSIONAL WAVE TURBULENCE

Vladimir ZAKHAROV — Landau Institute for Theoretical Physics, Moscow (Russia) + University of Arizona

Frédéric DIAS — Ecole Normale Supérieure de Cachan (France)

Andrei PUSHKAREV — Waves and Solitons LLC

(Philippe GUYENNE — McMaster University
Oleg VASILIEV — Landau Inst.)

November 2003 - Toronto

Workshop on Patterns in Physics

Introduction

A lot of physical problems involve random nonlinear dispersive waves. The most common tool for the statistical description of these waves is a kinetic equation for squared wave amplitudes.

The kinetic wave equation for water waves was derived by Hasselmann (1962) and Zakharov (1968).

Once the kinetic equation has been derived, the shape of wave number spectra can be predicted by the so-called weak turbulence theory.

Why weak? Because it deals with resonant interactions between small-amplitude waves

WT theory leads to explicit analytical solutions, provided some assumptions are made.

Few studies have been performed to check the validity of weak turbulence theory.

- Majda, MacLaughlin, Tabak [1997], + Cai [1999]
- Zakharov, Guyenne, Pushkarev, Dias [2001]
- Zakharov, Vasilyev, Dyachenko [2001]

J. Nonlinear Sci. Vol. 6: pp. 9–44 (1997)

Journal of Nonlinear Science

A One-Dimensional Model for Dispersive Wave Turbulence

A. J. Majda, D. W. McLaughlin, and E. G. Tabak

Courant Institute of Mathematical Sciences, New York University, 251 Mercer Street, New York, NY 10012, USA

Received July 16, 1996; manuscript accepted for publication August 15, 1996
Communicated by Stephen Wiggins

Summary. A family of one-dimensional nonlinear dispersive wave equations is introduced as a model for assessing the validity of weak turbulence theory for random waves in an unambiguous and transparent fashion. These models have an explicitly solvable weak turbulence theory which is developed here, with Kolmogorov-type wave number spectra exhibiting interesting dependence on parameters in the equations. These predictions of weak turbulence theory are compared with numerical solutions with damping and driving that exhibit a statistical inertial scaling range over as much as two decades in wave number.

It is established that the quasi-Gaussian random phase hypothesis of weak turbulence theory is an excellent approximation in the numerical statistical steady state. Nevertheless, the predictions of weak turbulence theory fail and yield a much flatter ($|k|^{-1/3}$) spectrum compared with the steeper ($|k|^{-3/4}$) spectrum observed in the numerical statistical steady state. The reasons for the failure of weak turbulence theory in this context are elucidated here. Finally, an inertial range closure and scaling theory is developed which successfully predicts the inertial range exponents observed in the numerical statistical steady states.

- relatively simple model (MMT)

$$i\frac{\partial\psi}{\partial t} = \left|\frac{\partial}{\partial x}\right|^{\alpha}\psi + \lambda\left|\frac{\partial}{\partial x}\right|^{\beta/4}\left(\left|\left|\frac{\partial}{\partial x}\right|^{\beta/4}\psi\right|^{2}\left|\frac{\partial}{\partial x}\right|^{\beta/4}\psi\right)$$

$$\lambda = \pm 1$$

Remark: if $\alpha = 2$, $\beta = 0$, one gets NLS

$\lambda = +1$: defocusing NLS

$\lambda = -1$: focusing NLS

In Fourier space, the MMT model looks like

$$i\frac{\partial \hat{\psi}_k}{\partial t} = \omega_k \hat{\psi}_k + \int T_{123k}\, \hat{\psi}_1 \hat{\psi}_2 \hat{\psi}_3^* \,\delta(k_1 + k_2 - k_3 - k)\, dk_1 dk_2 dk_3$$

Linear dispersion relation: $\omega_k = |k|^\alpha \qquad \alpha > 0$

Interaction coefficient: $T_{123k} = \lambda\, |k_1 k_2 k_3 k|^{\beta/4} \qquad (\lambda = \pm 1)$

PROPERTIES:

- Hamiltonian system: $i\frac{\partial \psi}{\partial t} = \frac{\delta H}{\delta \psi^*}$

  $H = H_L + H_{NL}$

- $N = \int |\psi|^2 dx$ is conserved (number of particles)
- $M = \frac{1}{2}\int (\psi \psi_x^* - \psi_x \psi^*)\, dx$ is conserved as well

RESONANT INTERACTIONS BETWEEN FOUR WAVES

$$k_1 + k_2 = k_3 + k$$
$$\omega_1 + \omega_2 = \omega_3 + \omega$$

(interesting case: $\alpha < 1$)

We take $\alpha = \frac{1}{2}$ (analogy with gravity waves)

USEFUL VARIABLE: $\eta(x,t) = \int_{-\infty}^{\infty} e^{ikx} \sqrt{\frac{\omega_k}{2}} \left(\hat{\psi}_k + \hat{\psi}_{-k}^* \right) dk$

WEAK TURBULENCE DESCRIPTION

The following approximations are made :

- random phase
- Gaussian statistics

The statistical behavior is described by the evolution of the two-point correlation function

$$\langle \hat{\psi}_k \, \hat{\psi}^*_{k'} \rangle = n(k,t)\, \delta(k-k')$$

The kinetic equation is given by

$$\frac{\partial n_k}{\partial t} = 4\pi \int |T_{123k}|^2 \left(n_1 n_2 n_3 + n_1 n_2 n_k - n_1 n_3 n_k - n_2 n_3 n_k \right)$$
$$\times\, \delta(\omega_1 + \omega_2 - \omega_3 - \omega)\, \delta(k_1 + k_2 - k_3 - k)\, dk_1\, dk_2\, dk_3$$

REMARK : independent on the sign of nonlinearity

Define : $N = \int n(k)\, dk$ number of particles

$E = \int \omega(k)\, n(k)\, dk$ quadratic energy

There are two types of stationary solutions of the kinetic equation :

- thermodynamic equilibrium
- Kolmogorov type $\longrightarrow$ $n \sim k^{-1}$

  constant flux of energy P

  $\longrightarrow$ $n \sim k^{-5/6}$

  constant flux of particles (

COLLAPSE

Solutions self-similaires (Self similar solutions)

$$\hat{\psi}(k,t) = (t_0 - t)^{p+i\varepsilon} \chi\left[k(t_0-t)^{1/\alpha}\right] \qquad p = \frac{\beta-\alpha+2}{2\alpha}$$

$\int_0^\infty |\hat{\psi}_k|^2 \, dk$ doit converger quand $k \to \infty$

$$\beta > \alpha - 1$$

Pour que H reste borné quand $t \to t_0$, il faut

$$\lambda = -1$$

Pour que $\hat{\psi}(k,t)$ reste borné quand $t \to t_0$, il faut que $\chi(\xi) \sim C\,\xi^{\frac{-\beta+\alpha-2}{2}}$ $\quad \xi \to 0$

$$\beta < \alpha$$

Lorsque ces conditions sont réunies,

collapse = formation d'une singularité intégrable dans le plan physique

Spectre : $n_k \sim |\hat{\psi}_k|^2 \sim |k|^{-\beta+\alpha-2}$

(analogie avec le spectre de Phillips)

QUASISOLITONS

True solitons

$\omega^2 = g|k| + \sigma|k|^3$

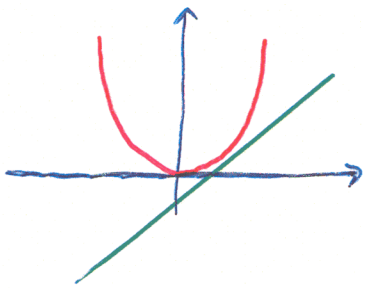

$\omega = |k|^\alpha$

$\alpha > 1$

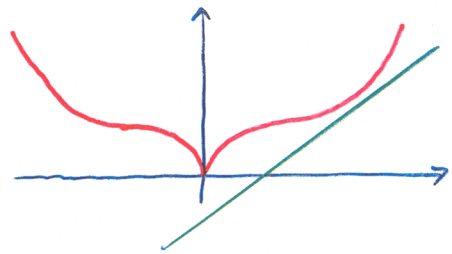

No true solitons

$\omega = |k|^\alpha \quad \alpha < 1$

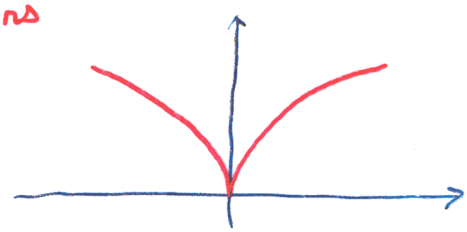

Quasisolitons

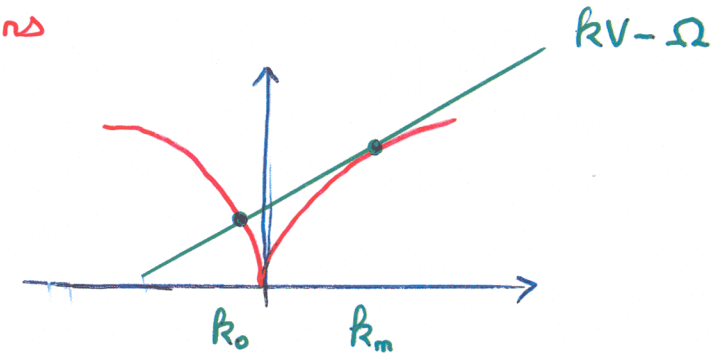

Solution of form $\Psi(x,t) = e^{i\Omega t}\xi(x - Vt)$

$\rightarrow$ denominator : $-\Omega + kV - |k|^\alpha$

NUMERICAL RESULTS

The equation $i \frac{\partial \hat{\psi}_k}{\partial t} = \omega(k) \hat{\psi}_k + \int T_{123k} \cdots dk_1 \, dk_2 \, dk_3$

$$+ i \left[F(k) + D(k) \right] \hat{\psi}_k$$

was integrated numerically (pseudospectral + 4th order Runge-Kutta). Up to 4096 de-aliased modes were used.

Typical initial conditions are random noise.

1> focusing $\lambda = -1$ $\alpha = \frac{1}{2}$ $\beta = 0$

2> focusing $\lambda = -1$ $\alpha = \frac{1}{2}$ $\beta = 3$

3> defocusing $\lambda = 1$ $\alpha = \frac{1}{2}$ $\beta = 0$

4> defocusing $\lambda = 1$ $\alpha = \frac{1}{2}$ $\beta = 3$

Comparison of the turbulence levels and fluxes of particles Q^+ for $\lambda = \pm 1$ leads to a paradoxal result.

At $\lambda = -1$, the total number of particles N is three times less than at $\lambda = +1$, while the dissipation rate of particles is higher by one order of magnitude.

Explanation: wave collapse, which is a powerful mechanism of nonlinear interactions, providing fast transport of wave particles to high frequencies.

(no violation of energy conservation)

The contribution of collapses to the high-frequency part of the spectrum is weak, because they produce Phillips-type spectra $n_k \sim k^{-3/2}$, steeper than Kolmogorov spectra.

(experiments with $\beta = 0$, $\alpha = \frac{1}{2}$)

COLLAPSE PHENOMENON

PHÉNOMÈNE DE COLLAPSE

$\beta = 0$, $\lambda = -1$ (focusing)

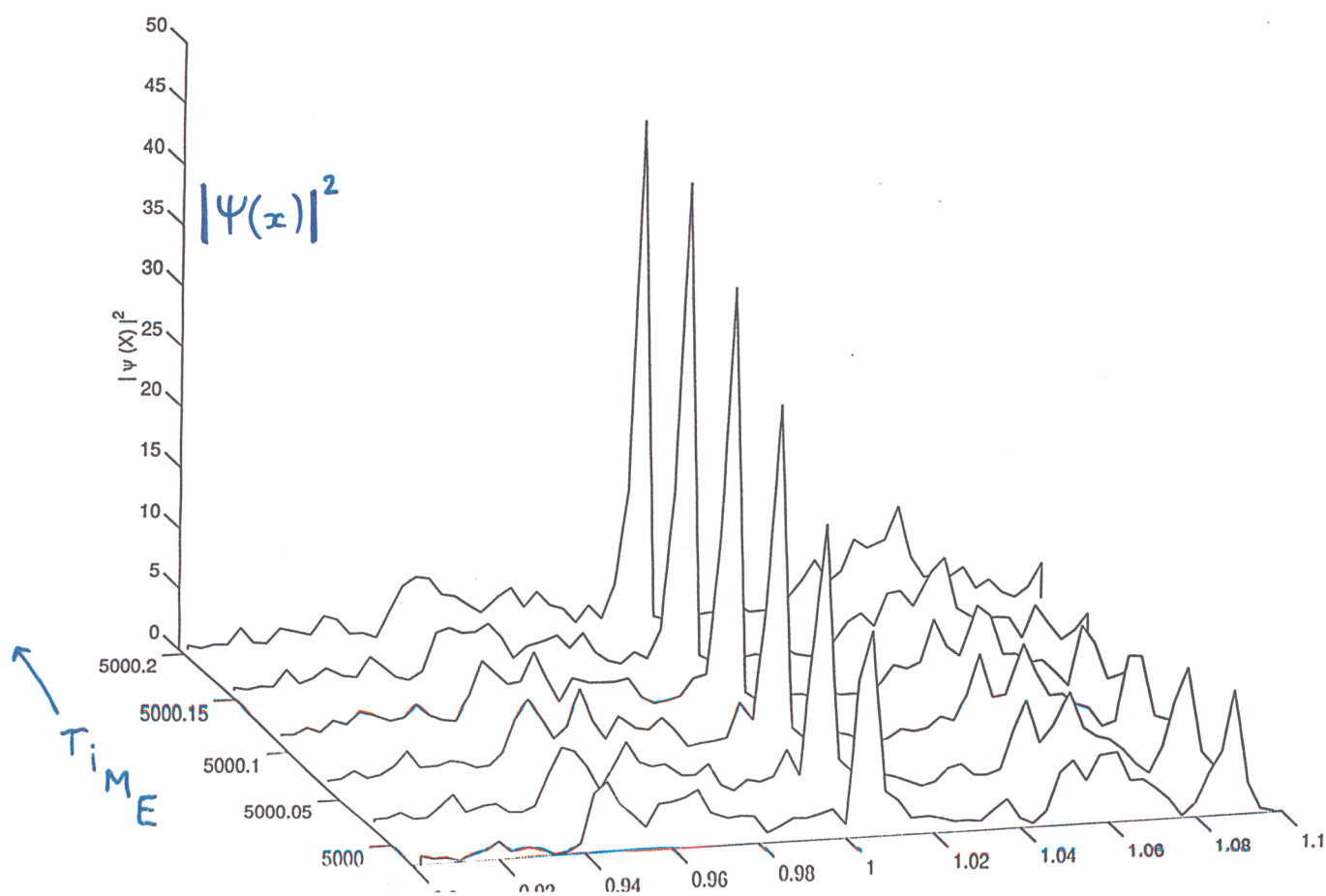

$\beta = 0 \quad \lambda = -1$ (focusing)

$|FT(\Psi_{200})|^2$

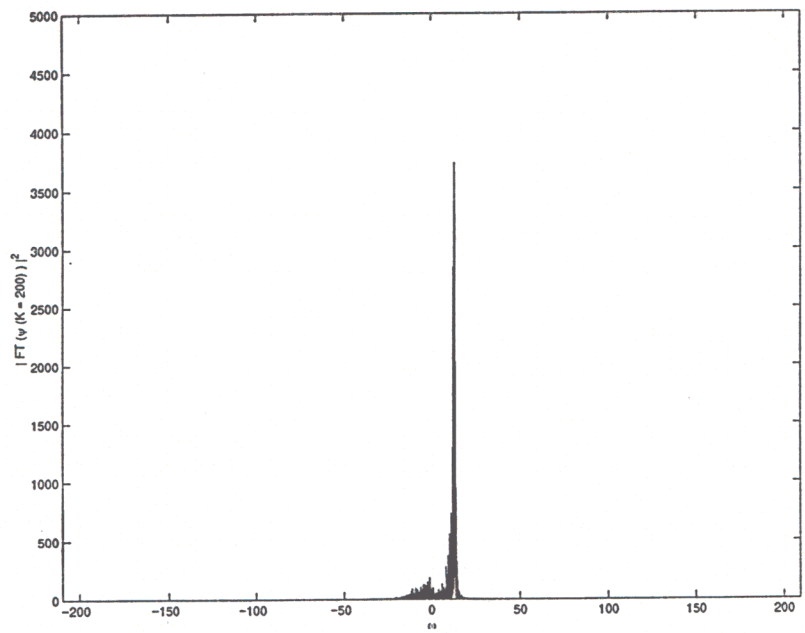

$\omega_{lin} = \sqrt{200}$
~ 14

nonlinear frequency shift

Figure 9: $\beta = 0, \lambda = -1$. Square amplitude of the Fourier transform for the mode $k = 200$ vs. frequency (time resolution $\tau = 0.015$).

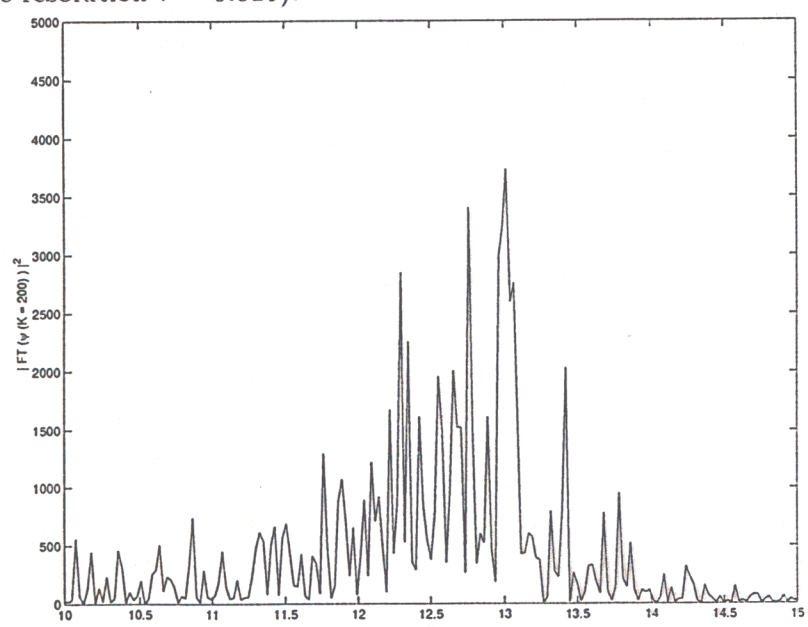

Figure 10: $\beta = 0, \lambda = -1$. Same as before but with a zoom on a smaller frequency window.

SINGULARITY FORMATION

conservative evolution

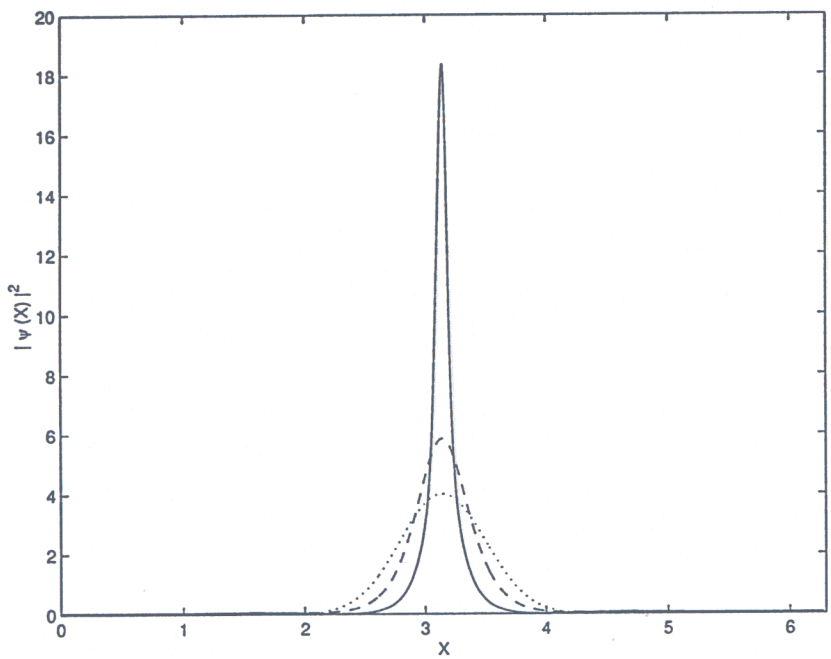

$\lambda = -1$

focusing

Figure 23: $\beta = 0, \lambda = -1$. Evolution towards a collapsing peak of the isolated solution for the initial amplitude $\psi_0 = 2$. Dotted line $t = 0$, dashed line $t = 0.55$, solid line $t = 1.1$.

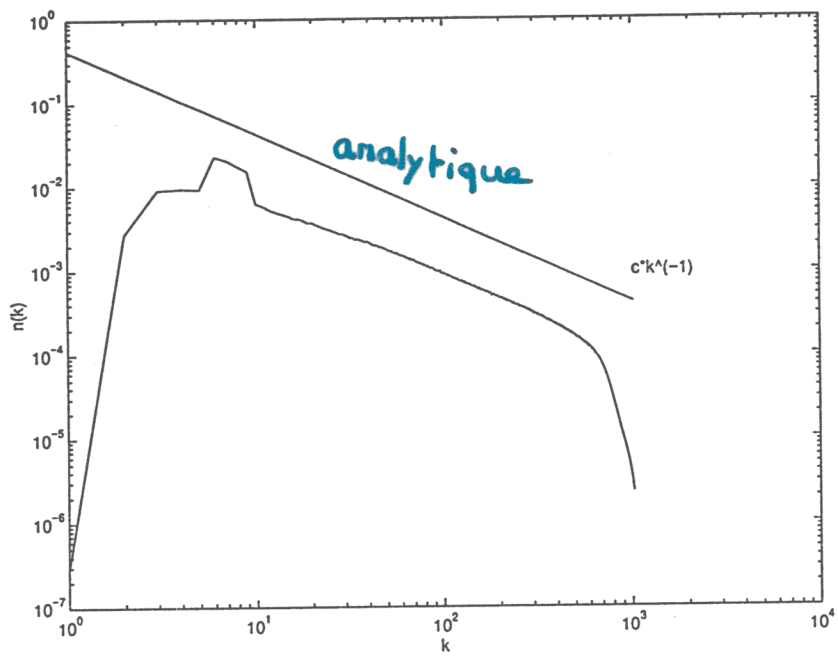

Figure 27: $\beta = 0, \lambda = -1$. Computed spectrum and WT spectrum vs. wave number. The WT spectrum (straight line) is given by $n(k) = c\,k^{-1}$ with $c = a\,P^{1/3} \simeq 0.42$.

SUPERCRITICAL WAVE TURBULENCE AND SELF-ORGANIZED CRITICALITY IN THE FOCUSING MMT MODEL

$(\lambda = -1)$

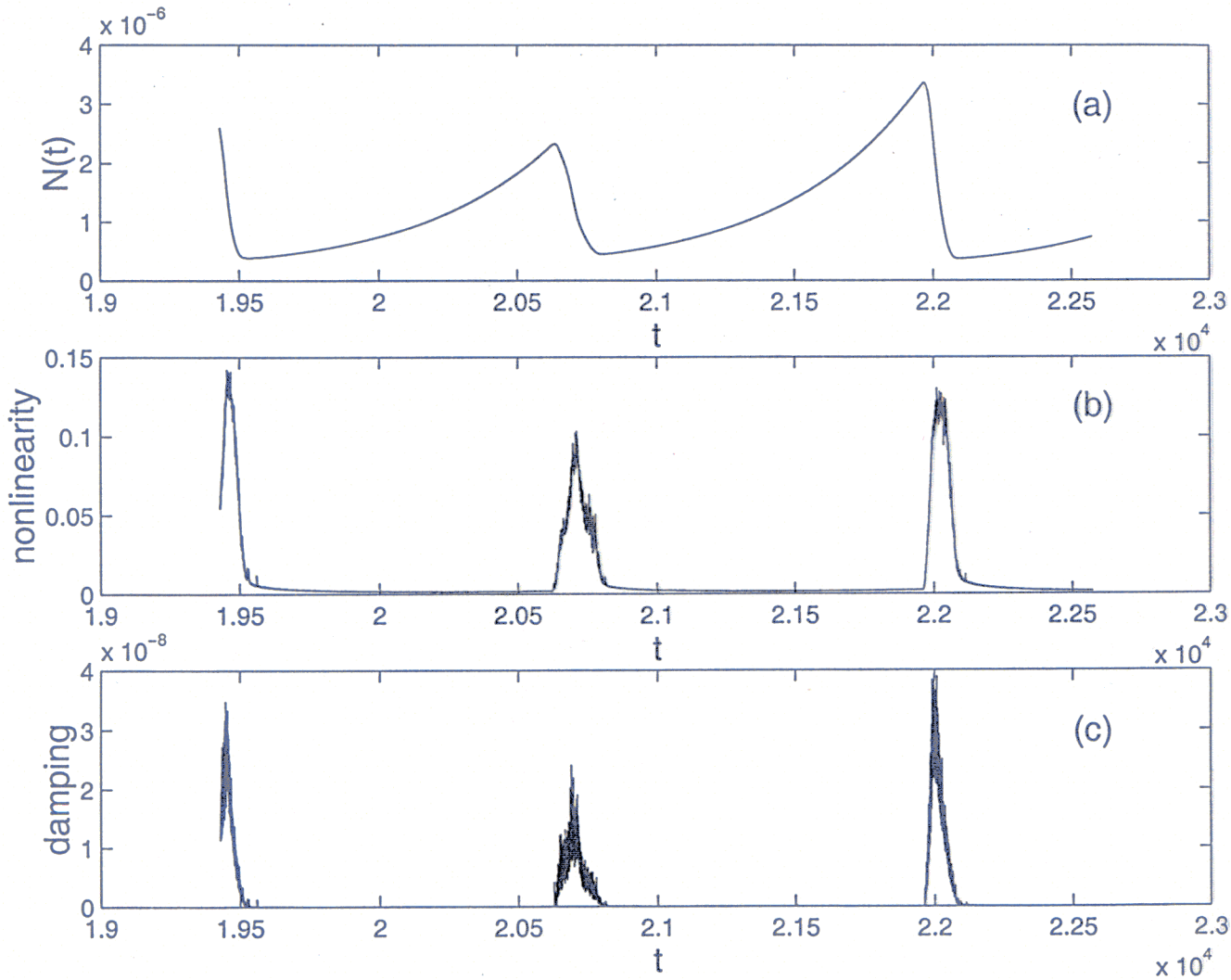

$\alpha = \frac{1}{2} \quad \beta = 3$

We see a chain of sporadic outbursts

FOCUSING CASE

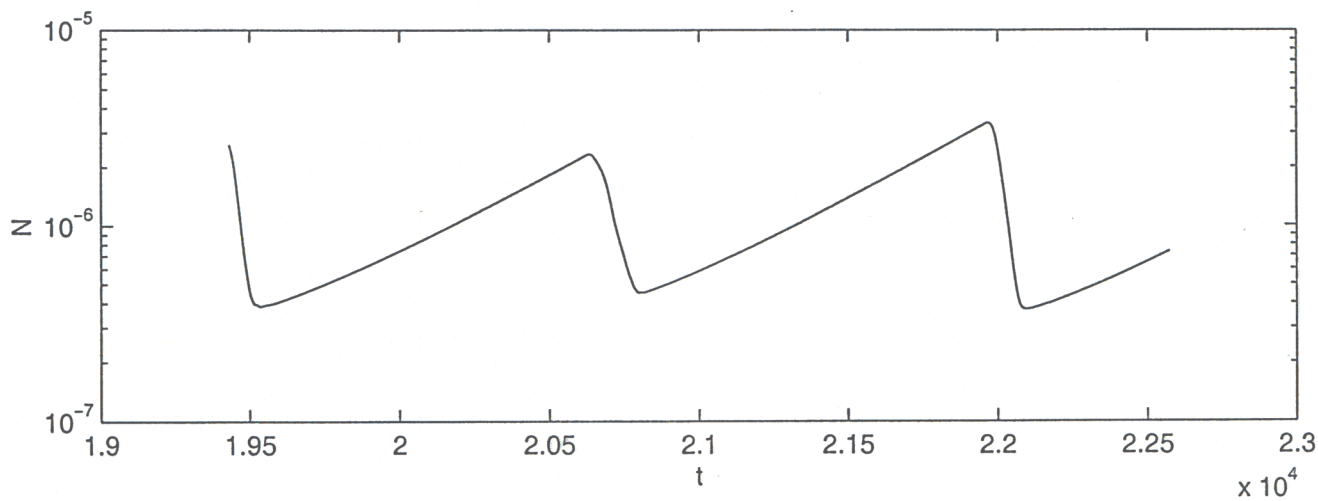

Wave amplitude grows almost exponentially

$|\Psi(x)|^2$ as a function of x

SUCCESSIVE TIMES

FOCUSING

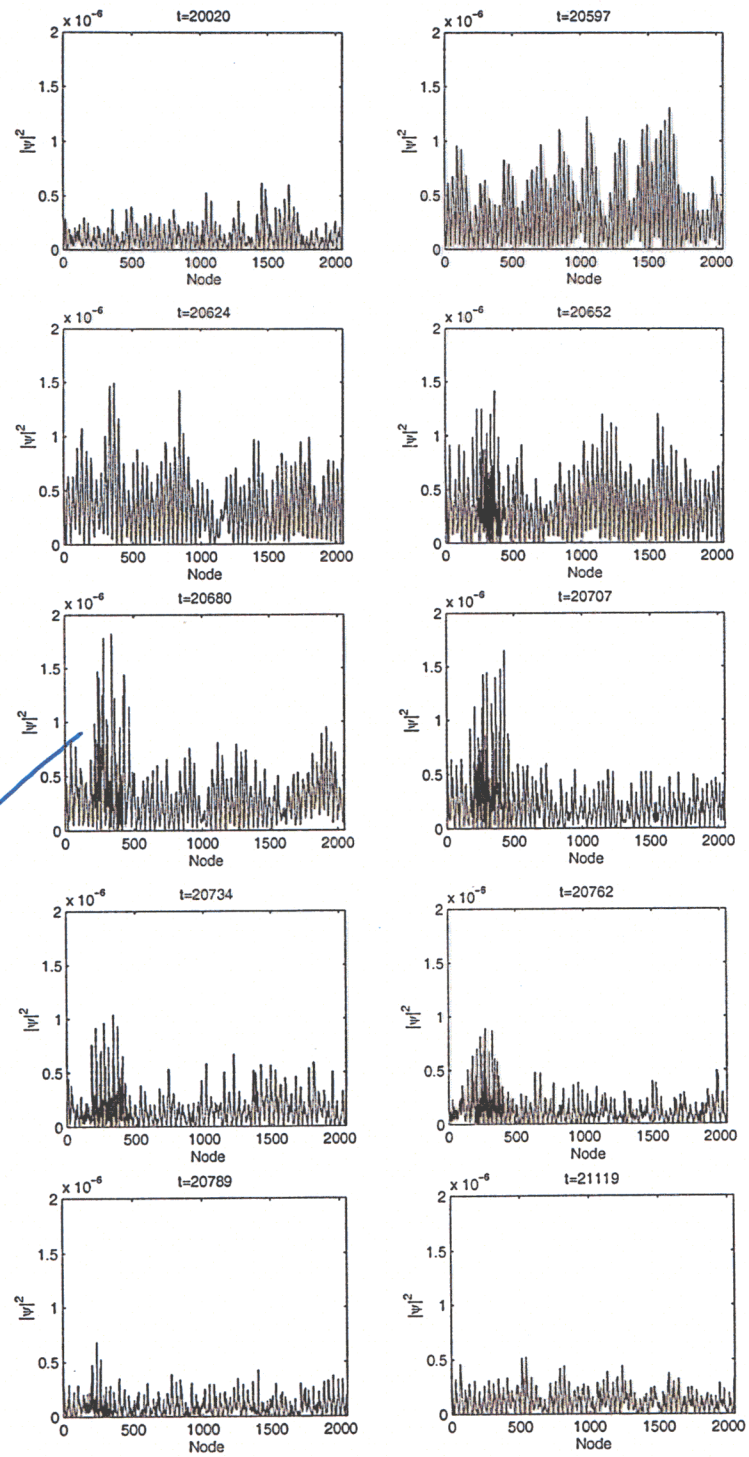

short wave instability

broad collapse

Fig. 13. Focusing MMT model ($\lambda = -1$) with $\alpha = 1/2, \beta = 3$. Plots of $|\psi(x)|^2$ versus x at successive times close to the moment of the first maximum of $N(t)$. The actual value of $x \in [0, 2\pi]$ is $x = \text{Node} \times (2\pi/N_d)$.

FOCUSING CASE

ZOOM OF THE REGION OF BROAD COLLAPSE

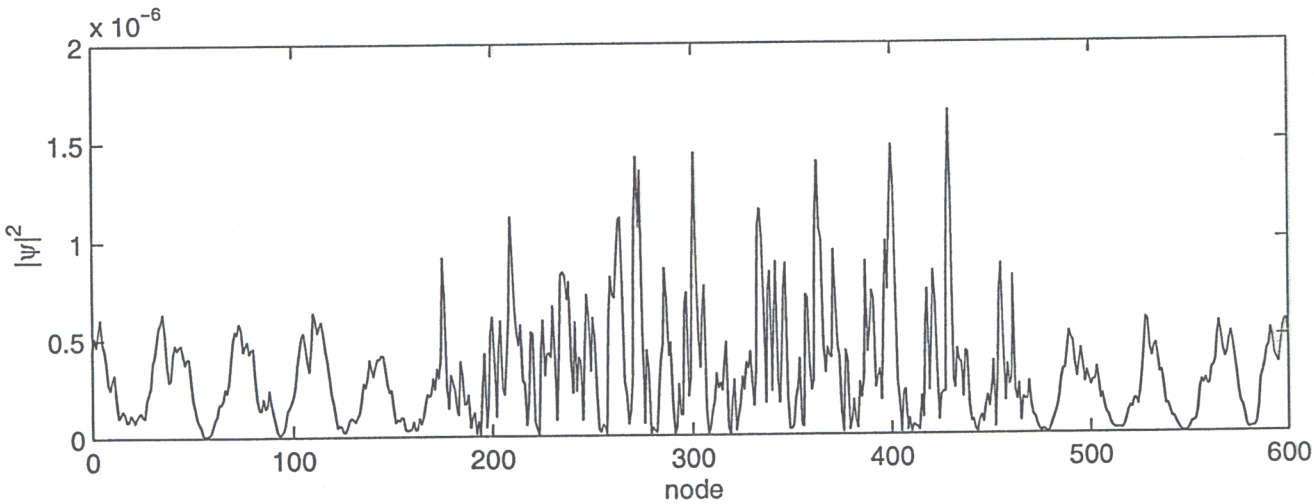

SPECTRUM

DEFOCUSING CASE

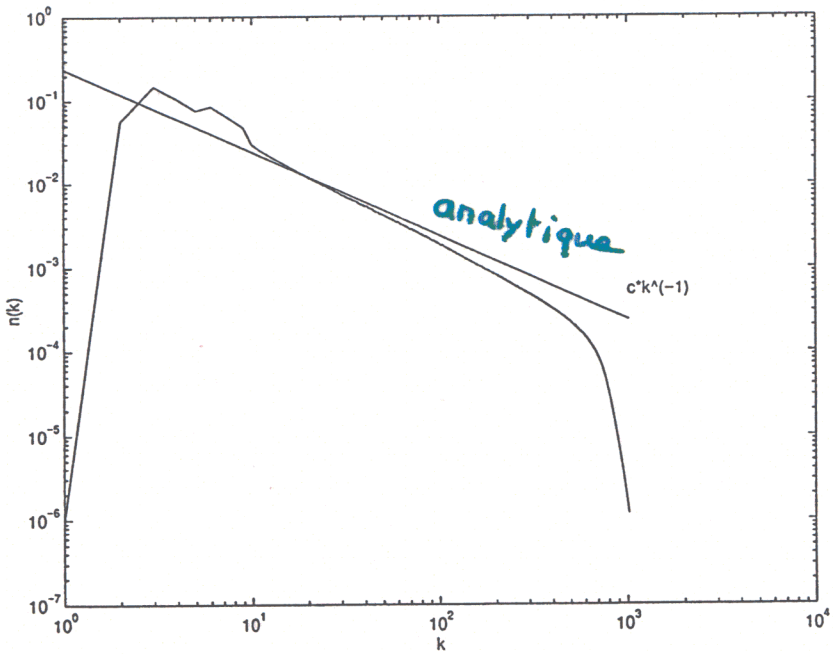

positive nonlinearity

Figure 28: $\beta = 0, \lambda = +1$. Computed spectrum and WT spectrum vs. wave number. The WT spectrum (straight line) is given by $n(k) = c\,k^{-1}$ with $c = a\,P^{1/3} \simeq 0.24$.

DEFOCUSING MMT MODEL

$(\lambda = 1)$

$\beta = 0 \quad \alpha = \frac{1}{2}$

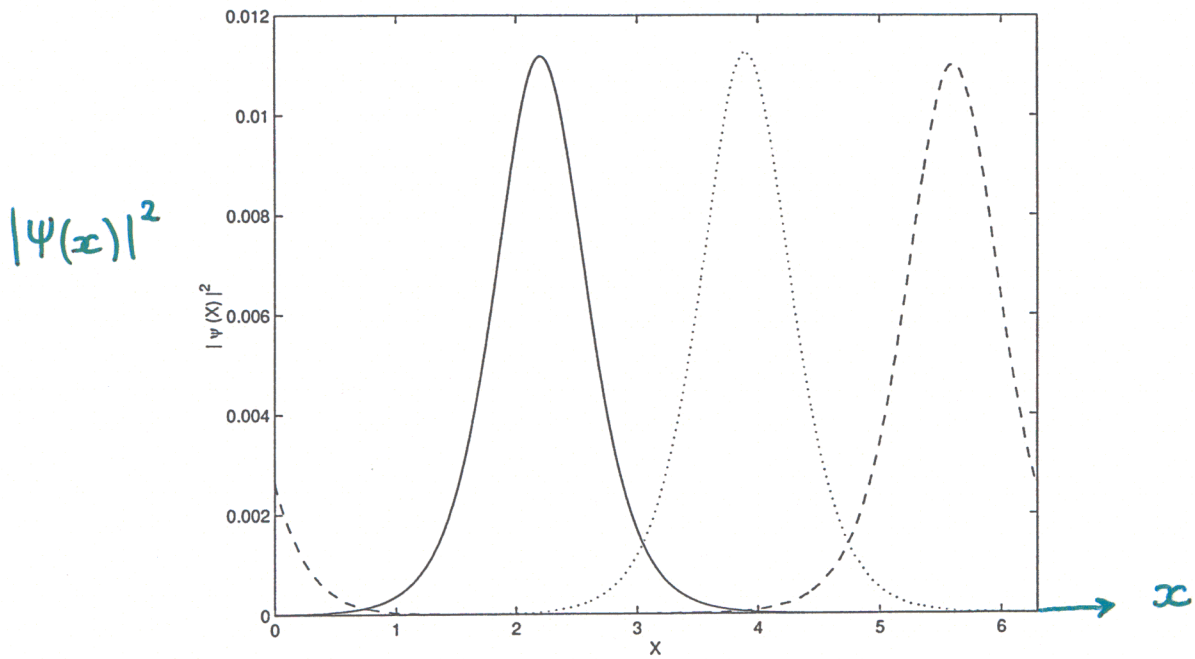

Figure 29: $\beta = 0, \lambda = +1$. Evolution of the initial quasisoliton for $q/k_m = 0.1$. Solid line $t = 0$, dotted line $t = 1250$, dashed line $t = 2500$.

evolution of a small amplitude quasisoliton (envelope)

DEFOCUSING MMT MODEL

$\lambda = 1 \qquad \alpha = 1/2 \qquad \beta = 0$

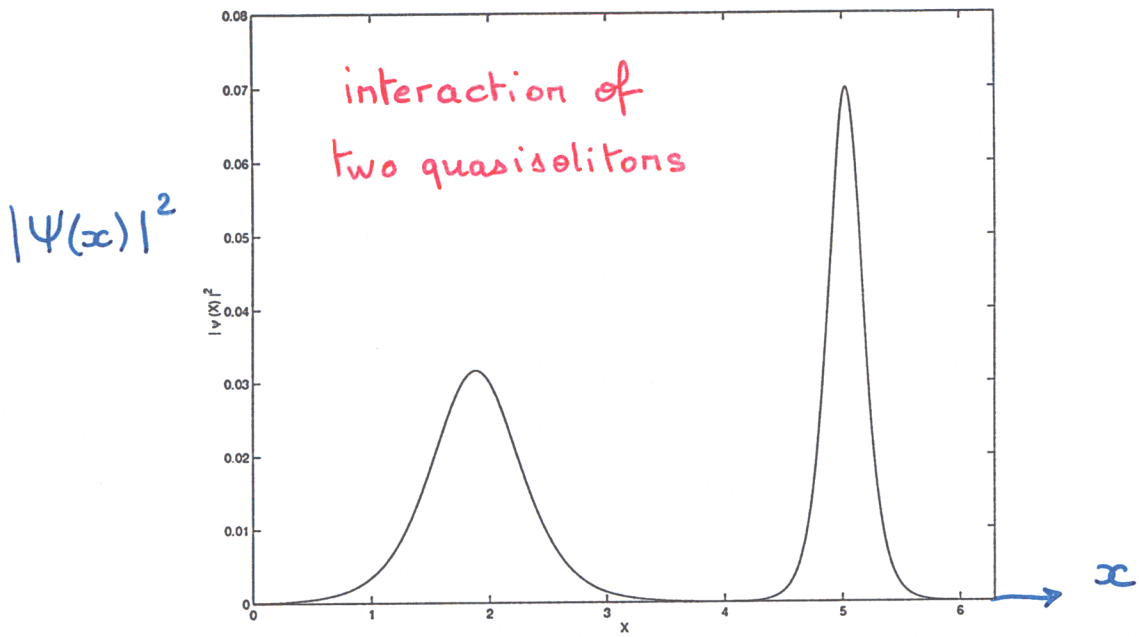

Figure 30: $\beta = 0, \lambda = +1$. Interaction of two initial quasisolitons at $t = 0$. The smaller and bigger ones correspond to $q/k_m = 0.2$ and 0.25 respectively.

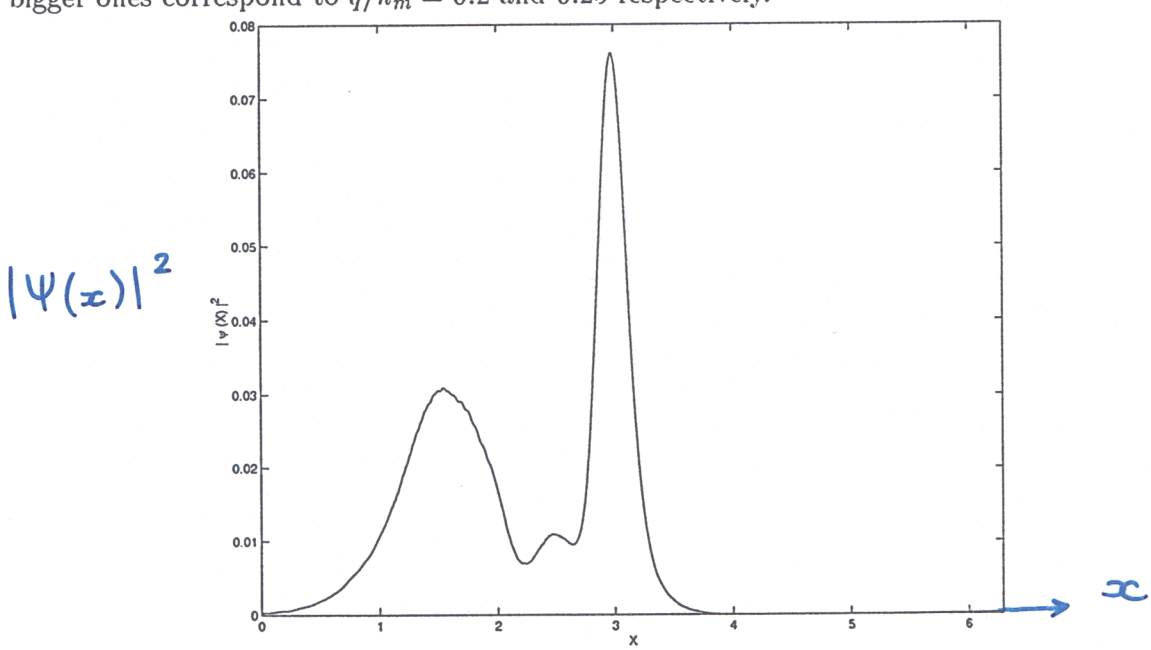

Figure 31: $\beta = 0, \lambda = +1$. Interaction of two initial quasisolitons at $t = 37.5$.

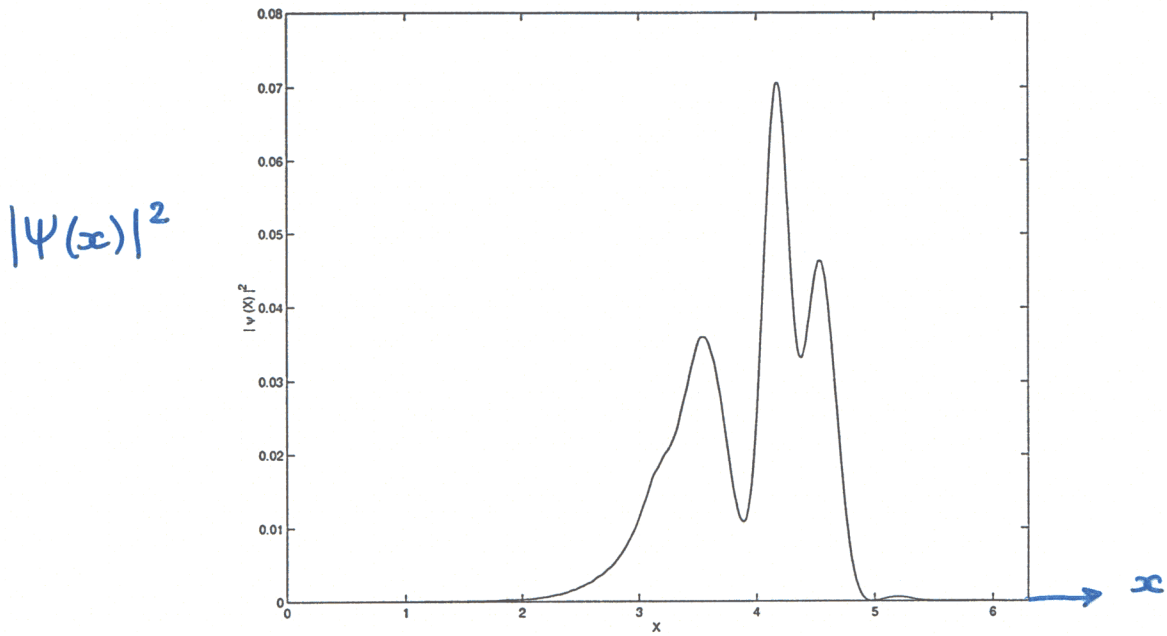

Figure 32: $\beta = 0, \lambda = +1$. Interaction of two initial quasisolitons at $t = 50$.

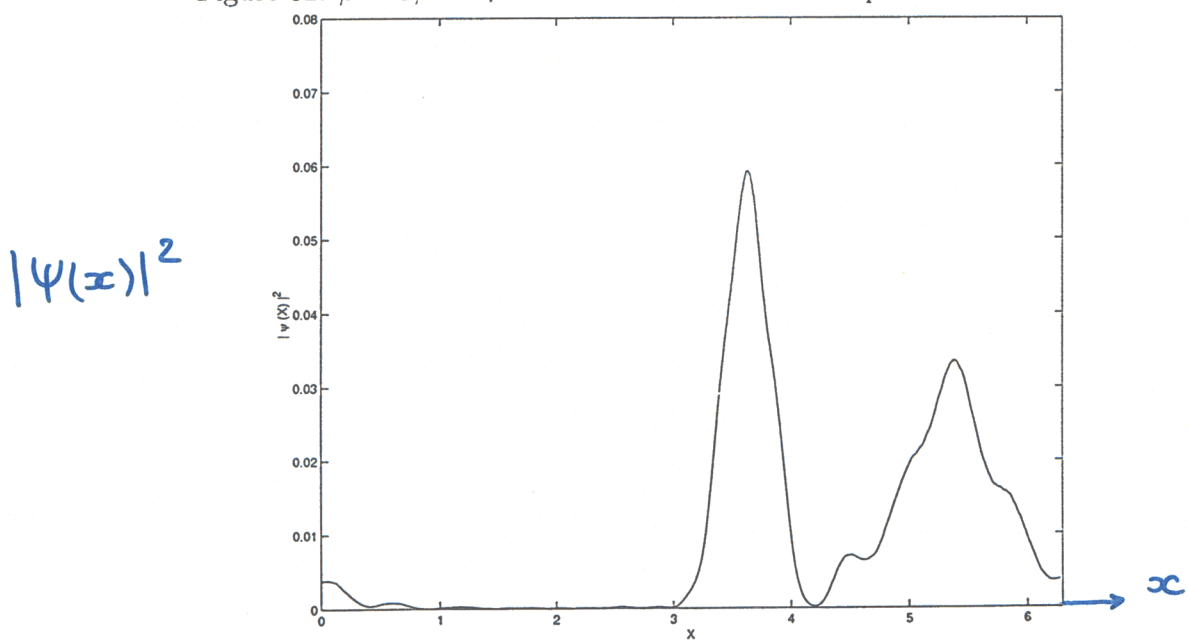

Figure 33: $\beta = 0, \lambda = +1$. Interaction of two initial quasisolitons at $t = 100$.

We performed computations with $\beta = +3$ (kernel for gravity waves).

The MMT equation was integrated with different kinds of initial conditions: random noise or single harmonic excitation. The later stages of evolution are strikingly similar. The wave system was separated into several soliton-like moving structures and low amplitude quasi-linear waves.

Interactions of solitons and waves slowly redistributed the number of waves. Bigger solitons grow while smaller solitons collapse.

Finally: one moving soliton + quasi-linear waves

DEFOCUSING MMT MODEL

propagation of quasi soliton

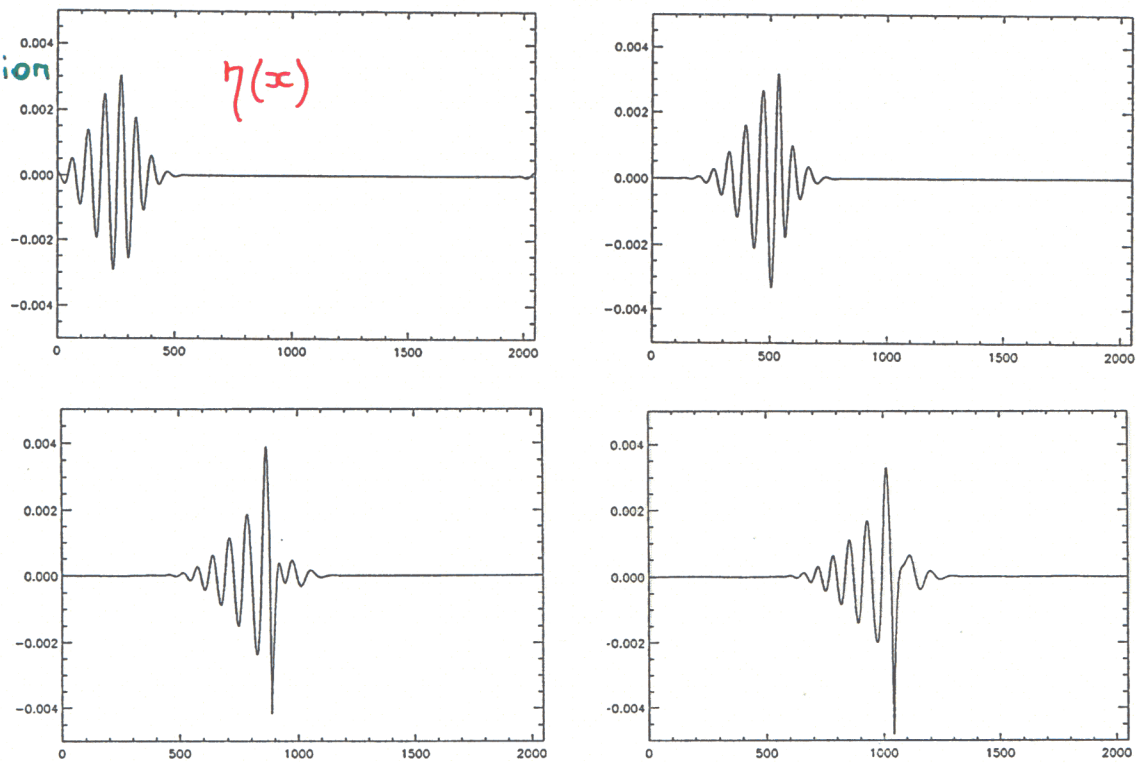

$\beta = 3$

Fig. 19. Defocusing MMT model ($\lambda = 1$) with $\alpha = 1/2, \beta = 3$. Plot of $\eta(x)$, given by Eq. (2.13), versus x, showing the propagation of a quasisoliton with $q/k_m = 0.3$: (a) $t = 7.854$, (b) $t = 15.708$, (c) $t = 26.704$, (d) $t = 31.416$. The actual value of $x \in [0, 2\pi]$ is $x = (2\pi/N_d)x_{\text{graph}}$.

DEFOCUSING MMT MODEL

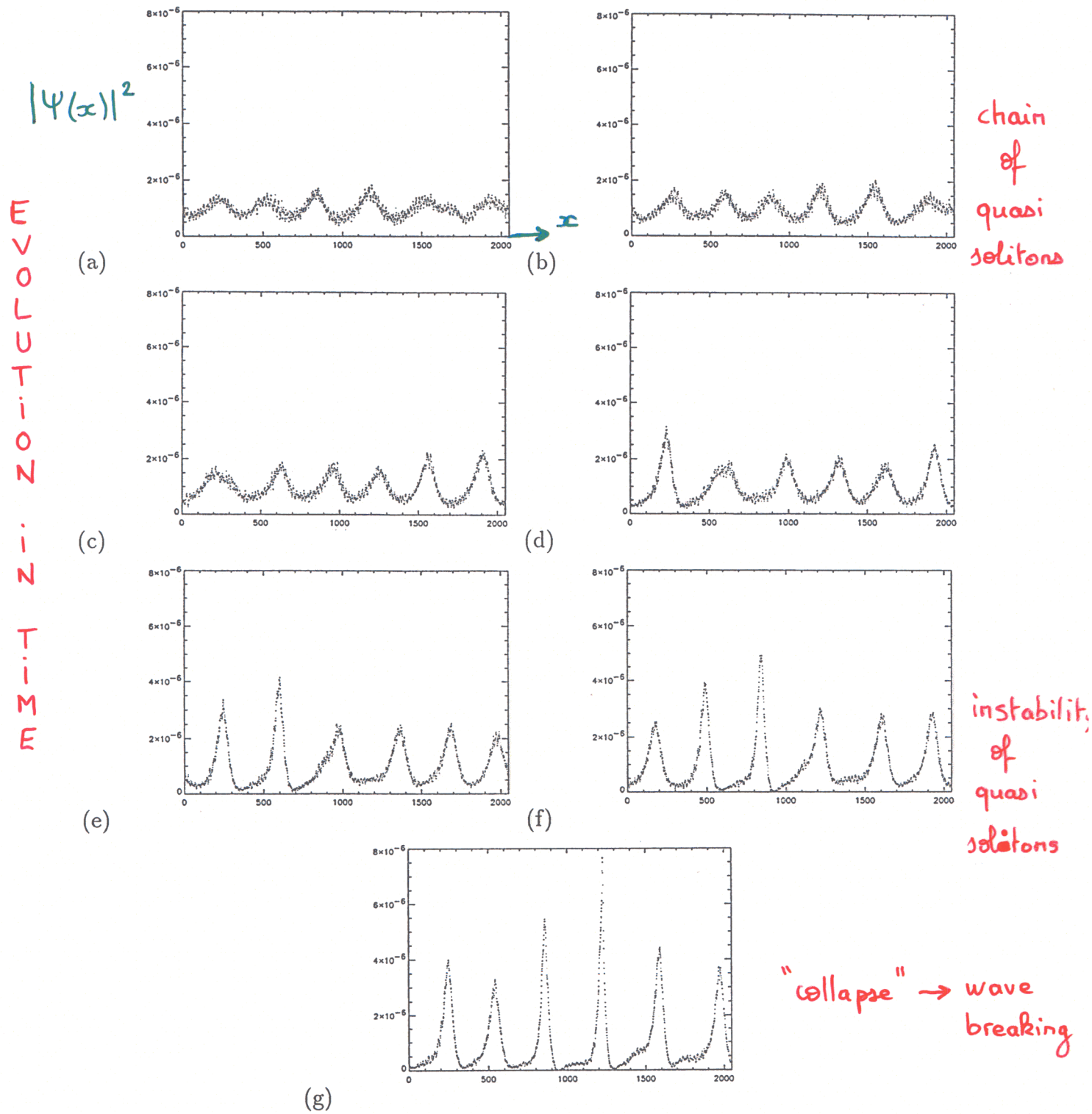

Fig. 21. Defocusing MMT model ($\lambda = 1$) with $\alpha = 1/2, \beta = 3$. Plot of $|\psi(x)|^2$ versus x, showing the development of the modulational instability. The monochromatic wave (10.1) is perturbed by (10.2). (a) $t = 349.502$, (b) $t = 361.283$, (c) $t = 373.064$, (d) $t = 384.845$, (e) $t = 396.626$, (f) $t = 404.480$, (g) $t = 416.261$. The actual value of $x \in [0, 2\pi]$ is $x = (2\pi/N_d)x_{\text{graph}}$.

DEFOCUSING MMT MODEL

MOVING SOLITON

forcing added

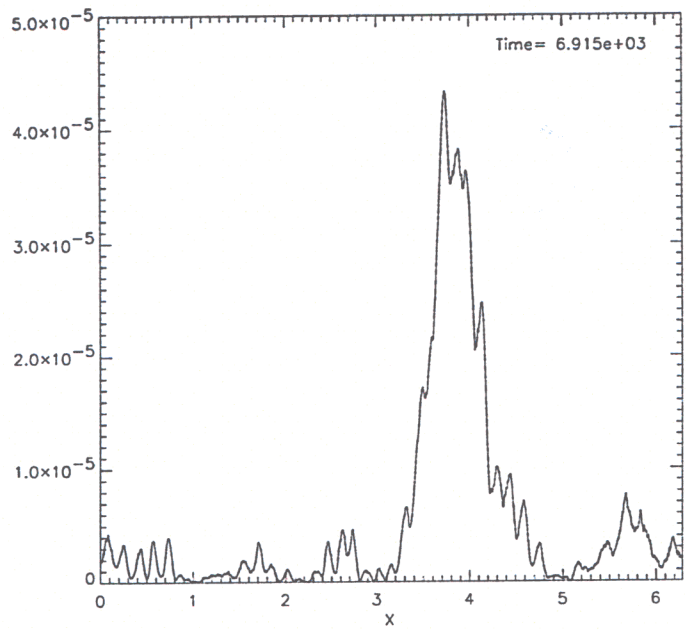

$\lambda = +1$

$\beta = 3$

Figure 34: $\beta = 3, \lambda = +1$. Single moving soliton, $t = 6915$.

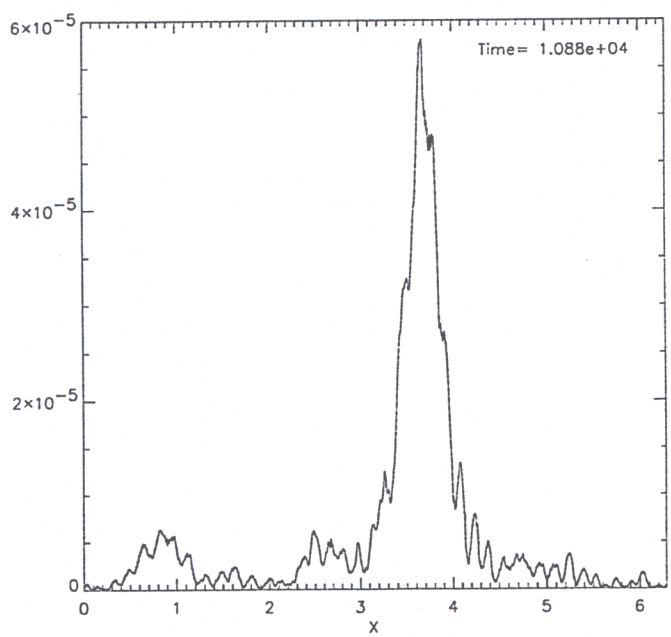

Figure 35: $\beta = 3, \lambda = +1$. Single moving soliton, $t = 10880$.

DEFOCUSING MMT MODEL

$(\lambda = 1)$

$\alpha = 1/2 \qquad \beta = 3$

(forcing + damping)

~ wind for water waves

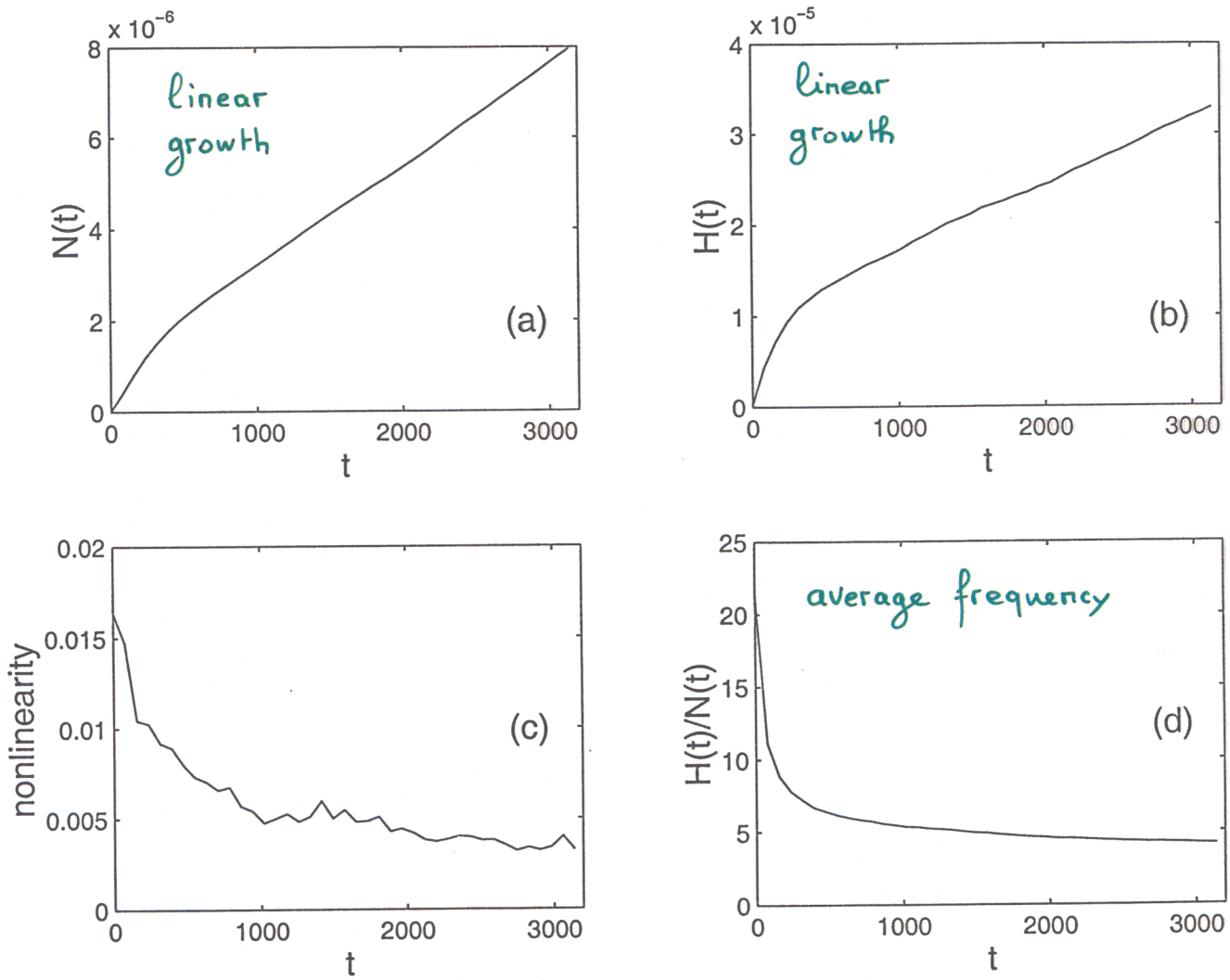

DEFOCUSING MMT MODEL

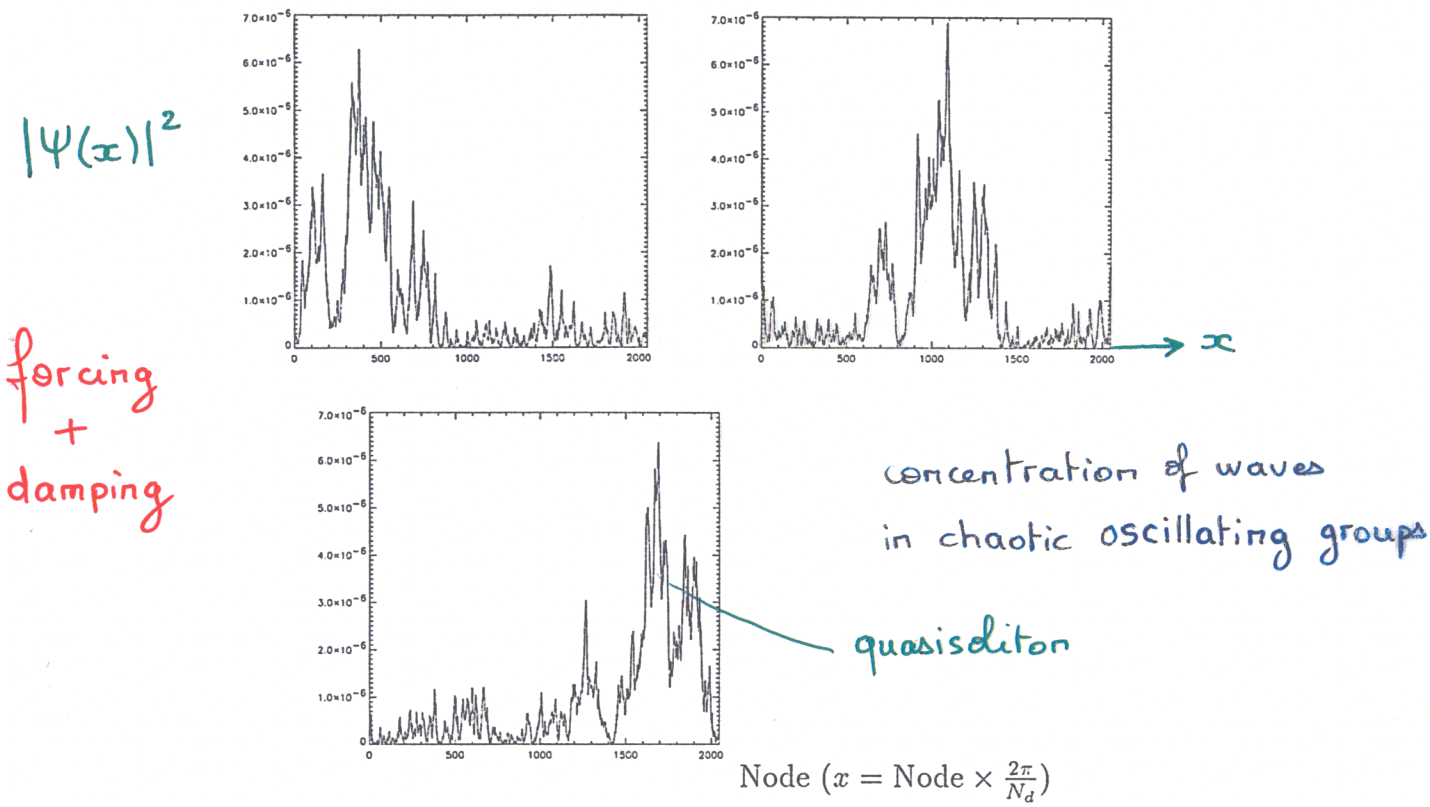

Fig. 24. Defocusing MMT model ($\lambda = 1$) with $\alpha = 1/2, \beta = 3$ in the presence of forcing and damping. Plot of $|\psi(x)|^2$ versus x. (a) $t = 2358.16$, (b) $t = 2373.87$, (c) $t = 2389.57$. The actual value of $x \in [0, 2\pi]$ is $x = (2\pi/N_d)x_{\text{graph}}$.

DEFOCUSING MMT MODEL

spatial distribution of energy damping

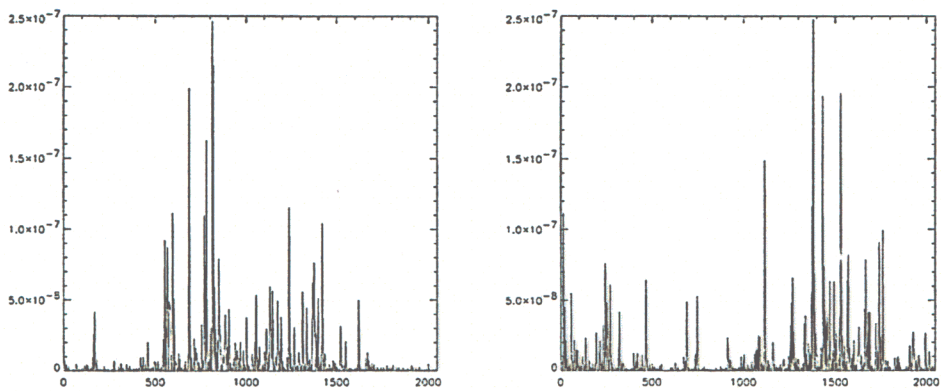

$(\lambda = 1)$

$\alpha = 1/2 \quad \beta = 3$

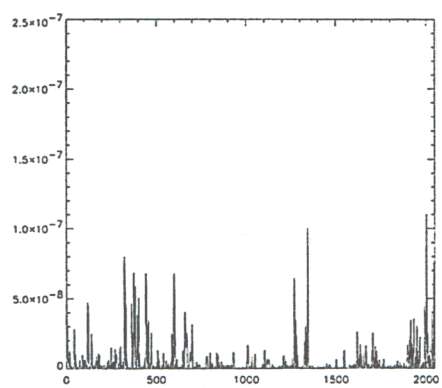

forcing + damping

Fig. 26. Defocusing MMT model ($\lambda = 1$) with $\alpha = 1/2, \beta = 3$ in the presence of forcing and damping. Evidence of intermittency. Plot of $\Gamma(x)$ versus x. $\Gamma(x)$ is defined by (10.3). (a) $t = 2358.16$, (b) $t = 2373.87$, (c) $t = 2389.57$. The actual value of $x \in [0, 2\pi]$ is $x = (2\pi/N_d)x_{\text{graph}}$.

EARLY STAGE

DEFOCUSING MMT MODEL

- not only downwind waves are present (also upwind waves)
  ↓
  four wave interaction
- rough spectrum

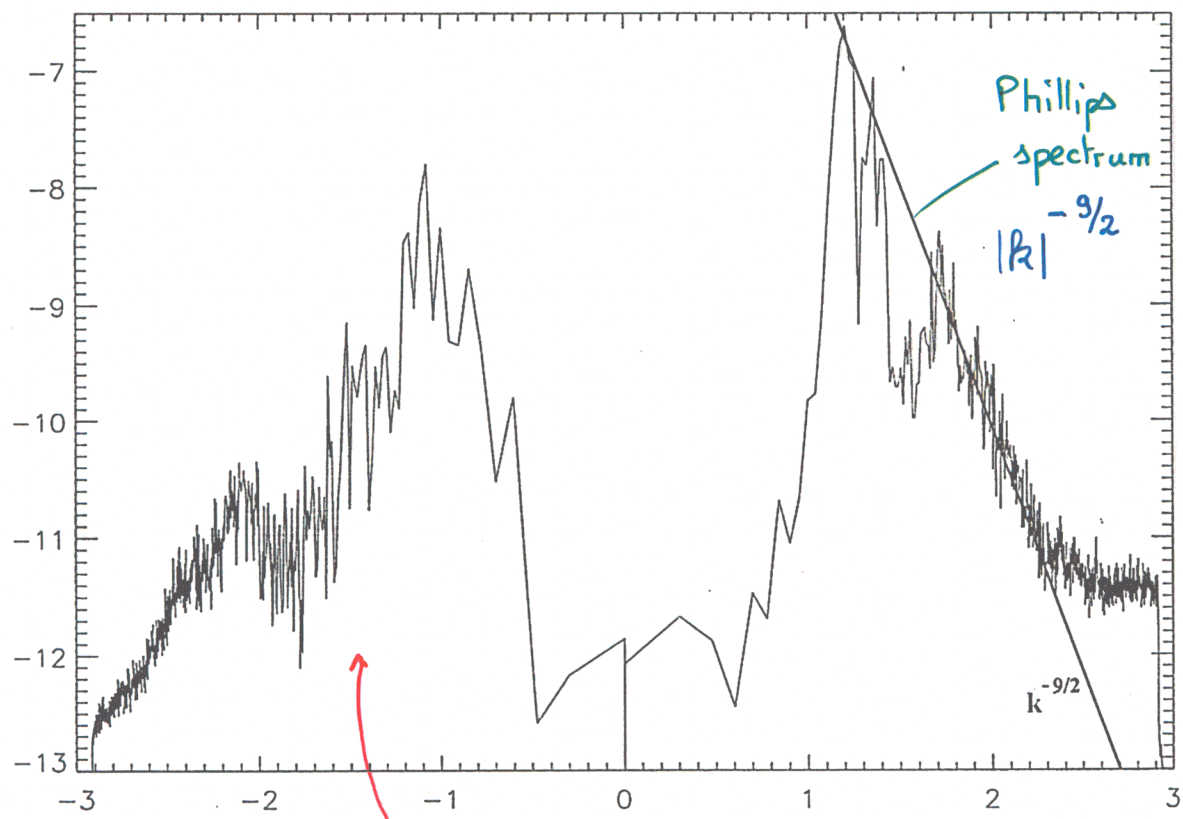

KOLMOGOROV SPECTRUM

for upwind component

LATER STAGE

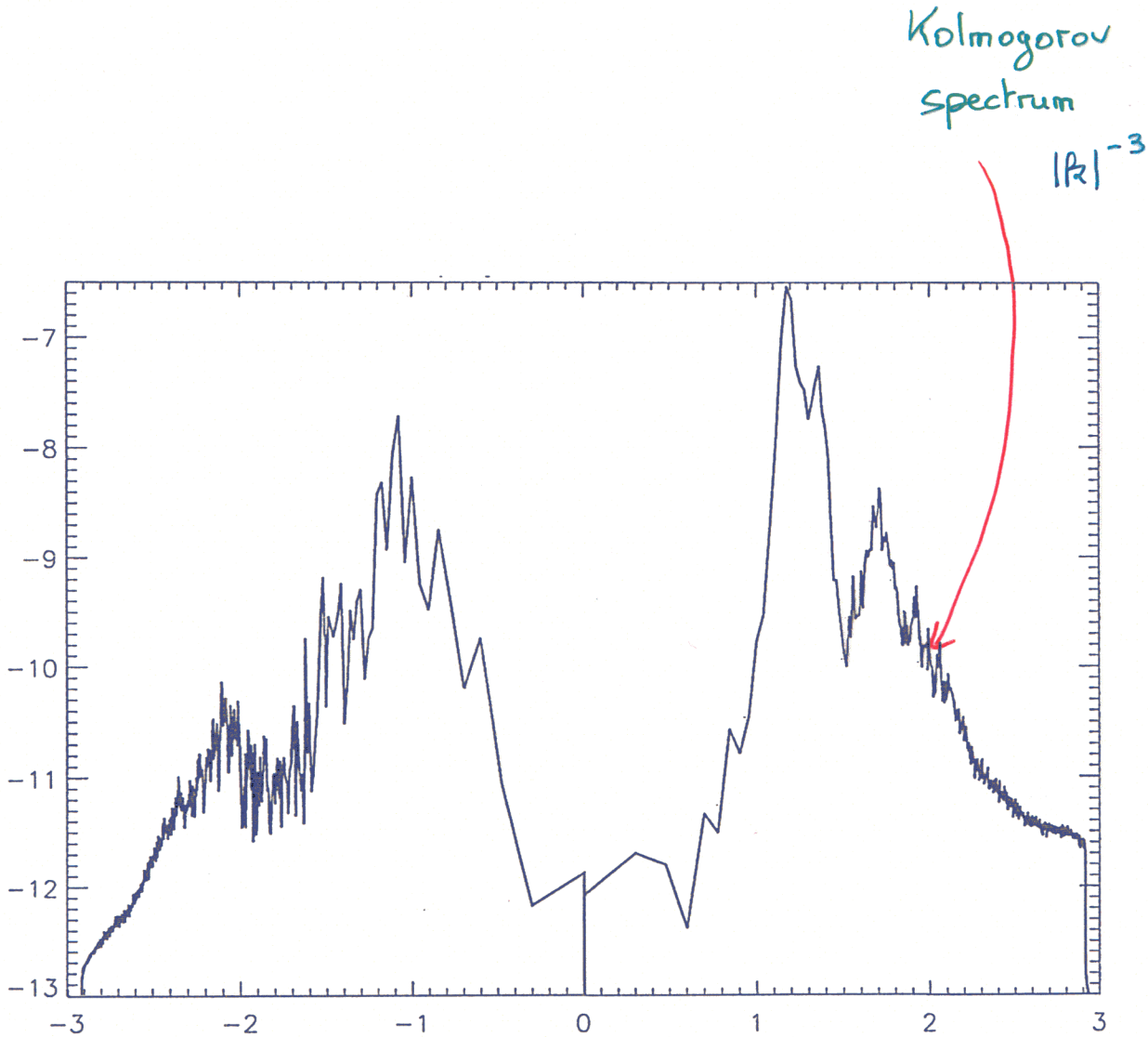

wave of maximum amplitude

$ka \approx 0.6$

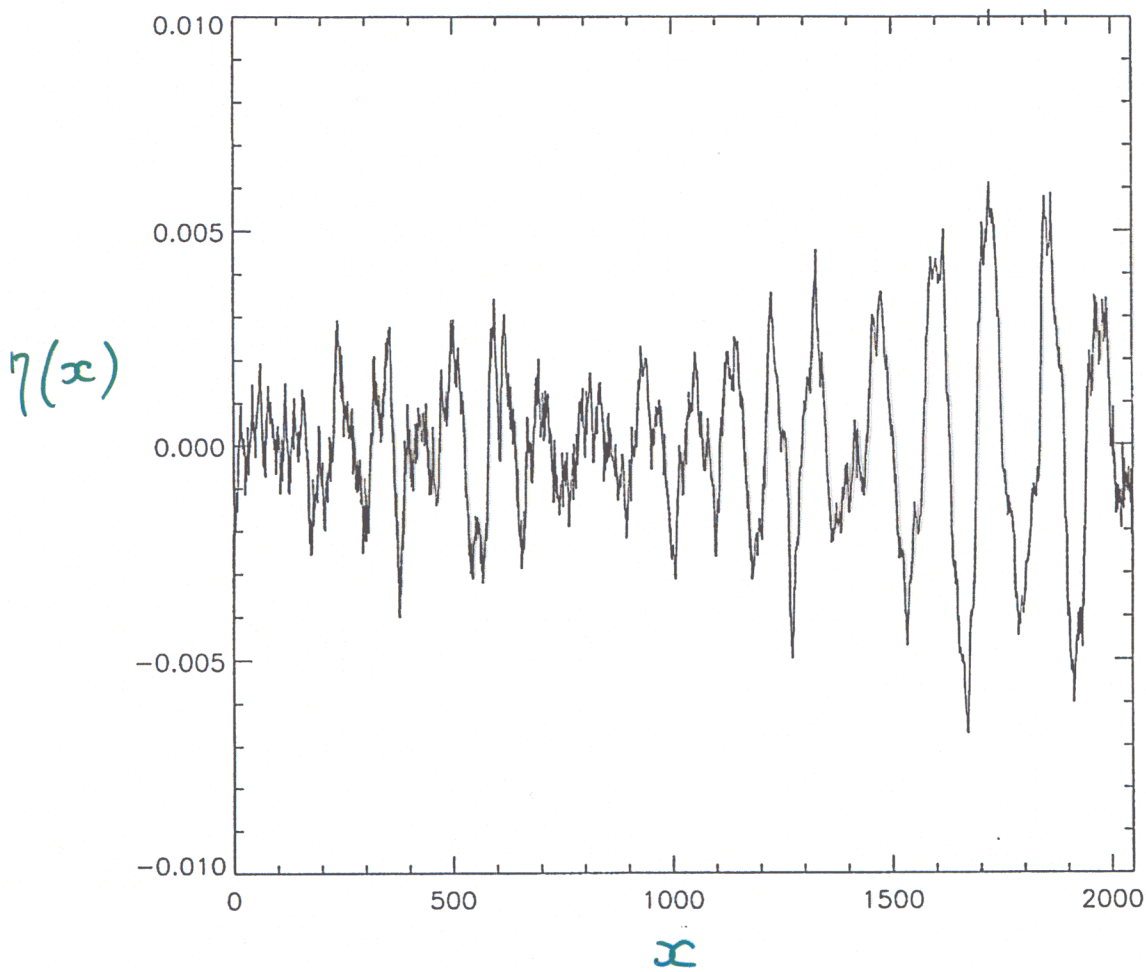

FREAK WAVE ?

SCENARIO FOR QUASISOLITONIC TURBULENCE

Generation of waves (short) by wind

↓

Formation of quasisolitons (initially small)

↓

Merging of quasisolitons and formation of large quasisolitons

↓

Instability of large qs and appearence of collapses (wave breaking)

↓

formation of direct cascade

↓

"equilibrium" is achieved at large k

at small k: growth of energy and slow downshift